The first evaluation of diagenesis rate of ancient bones by laser- induced breakdown spectroscopy (LIBS) in archaeological context prior to radiocarbon dating

Xueshi Bai, Apolline Pin, Jingjun Lin, Maxime Lopez, Corinna Dandolo, Pascale Richardin, Vincent Detalle

The first evaluation of diagenesis rate of ancient bones by laser-induced breakdown spectroscopy (LIBS) in archaeological context prior to radiocarbon dating

Xueshi Bai, Apolline Pin, Jingjun Lin, Maxime Lopez, Corinna Koch Dandolo, Pascale Richardin, Vincent Detalle

PII: S0584-8547(19)30112-0
DOI: https://doi.org/10.1016/j.sab.2019.04.007
Reference: SAB 5606

To appear in: *Spectrochimica Acta Part B: Atomic Spectroscopy*

Received date: 28 February 2019
Revised date: 10 April 2019
Accepted date: 11 April 2019

Please cite this article as: X. Bai, A. Pin, J. Lin, et al., The first evaluation of diagenesis rate of ancient bones by laser-induced breakdown spectroscopy (LIBS) in archaeological context prior to radiocarbon dating, Spectrochimica Acta Part B: Atomic Spectroscopy, https://doi.org/10.1016/j.sab.2019.04.007

The First Evaluation of Diagenesis Rate of Ancient Bones by Laser-Induced Breakdown Spectroscopy (LIBS) in Archaeological Context Prior to Radiocarbon Dating

Xueshi Bai[a, b], Apolline Pin[a], Jingjun Lin[c], Maxime Lopez[a, d], Corinna Koch Dandolo[a, d], Pascale Richardin[a, e], Vincent Detalle[a, *]

[a]*Centre for Research and Restoration of the Museums of France (C2RMF), 14 Quai François Mitterrand, 75001 Paris, France*

[b]*Centre de Recherche sur la Conservation (CRC), Muséum national Histoire naturelle, CNRS, Ministère de la Culture, 36 rue Geoffroy Saint Hilaire, 75005 Paris, France*

[c]*School of Electrical&Engineering, Changchun University of Technology, Changchun, Jilin, 120012, China*

[d]*Fondation des sciences du patrimoine / EUR-17-EURE-0021, 33, boulevard du Port MIR de neuville, 95011 Cergy-Pontoise, France*

[e]*CNRS - UMR 7055 – Préhistoire & Technologie, Maison Archéologie & Ethnologie René Ginouves, 21, allée de l'Université, 92023 Nanterre Cedex, France*

[*]*vincent.detalle@culture.gouv.fr*

Abstract

We provide in this study a new application of laser-induced breakdown spectroscopy (LIBS) to evaluate whether ancient bones contain sufficient organic material before radiocarbon dating, which can avoid a complex preliminary analysis on the samples or unnecessary sampling. We first examined the plasma induced by UV (266 nm) ns-laser on pellets of compressed bone powder, and in a second step the plasma induced on raw bones using different gas environment. Firstly, we carried out a common method of analyzing the organic material using LIBS by observing C-N band emission in Ar-He mixture environment, the sample of non-undergone significant diagenesis, which contents enough collagen, can be well discriminated for further

radiocarbon dating. Then spectral emission from nitrogen and carbon atoms was also recorded for these two types of samples in He and air environments. Calibration curves for carbon and nitrogen concentration of the bone were built to indicate the residual amount of collagen after undergoing the diagenesis (or degradation) and also to illustrate the possible carbonaceous pollution. The results proved that even if only several µg of material is analyzed for each laser shot, LIBS has a potential to carry out *in situ* measurements in archeological context while simultaneously performing a quantitative analysis.

Keywords: LIBS, Quantitative analysis, Ancient bones, Radiocarbon dating, Collagen content

Introduction

Radiocarbon dating has been a standard tool for archaeologists since the late 1940s [1]. The dating of ancient or archaeological bones is carried out on their organic fraction [2, 3], the collagen, which can be extracted according to the Longin method [4]. The most widely used technique today for radiocarbon dating is counting the number of ^{14}C and ^{12}C atoms in a given sample via accelerator mass spectrometry, which requires at least 0.5 mg of carbon to be extracted from collagen (corresponding to 1-3 g mechanically cleaned bone) to perform the measurement [5].

However, some bones have undergone a very important diagenesis due to their age, especially because of the environmental conditions of their burial [6]. The extremely degraded bones may therefore lack collagen, which makes performing radiocarbon dating impossible or very uncertain on these samples. This explains why preliminary analyses are generally carried out in order to determine the residual collagen concentration of a bone before extraction [7, 8]. These analyses determine the extent to which dating is possible and they enable the adaptation of the samples preparation protocols to the results. These preliminary analyses currently consist in the evaluation of the nitrogen (N wt%) and carbon (C wt%) concentration of the bones, which

provides access to the residual amount of collagen and any exogenous carbon pollution [9-12]. These analyses can usually be carried out by elemental analysis by flash combustion technique [13]. Attenuated total Reflectance-Fourier-transform infrared spectroscopy (ATR-FTIR) has been recently proposed to estimate the quantity of bone collagen content [14] by measuring the molecular band vibration. These techniques, however, require sampling on the bones, which affects their integrity and may cause aesthetic problems of particular relevance for museum pieces. The preparation for these analyses is burdensome, and it can also involve unnecessary removal of some parts of the bone considering that the results may show an absence of collagen and therefore indicate that the bones are impossible to date.

We propose a straightforward, versatile spectrochemical analysis technique, laser-induced breakdown spectroscopy (LIBS), in order to determine whether the residual organic fraction is sufficient for radiocarbon dating. The advantage of LIBS could be to provide an *in situ*, rapid, micro-destructive approach, performed directly on the sample while simultaneously reducing the analytical procedure [15,16]. LIBS especially offers an analytical ability for light elements identification and molecular band emission in the organic materials such as animal products, polymers, the products for heritage conservation like the mural painting (binder, adhesives, and consolidation products), etc. [17-20]. This work focuses on technical feasibility for the preliminary analysis before preforming radiocarbon dating for bone samples. According to our previous study [21], by observing the distribution of molecular emissions from CN, C_2 band in plasma, the nitrogen from air strongly contributed to the recombination with the C from the sample, which makes quantitative analysis difficult. Thus, we focused this present research on evaluating the possibility to get quantitative measurements by building a calibration curve as a function of the concentration of carbon and/or nitrogen in a given ambient gas in order to get rid of nitrogen in air. CN molecular emission and C and N elemental emissions are then used for determining the diagenesis rate in the ancient bone samples.

Material and preparation

Structure and Chemical Composition of Bones

At a macroscopic scale, bones consist of two parts: compact bone (cortical) and cancellous bone (trabecular) with high porosity. [22] At a microscopic scale, the external surface of the bone is covered by a thin fibrous membrane called the periosteum, with the exception of the joints which are covered with cartilage. The overall thickness of the compact bone may range from 0.7 mm to 10 mm, with a density of the order of 2 g/cm^3. [23-25] We are interested in this compact part because it is the most available and it is also much easier to analyze the external surface than the internal part. Besides, from the study of Z.A.Abdel-Salam, et. al, more material can be vaporized by laser into plasma from the hard part of bones and the temperature of plasma is higher, which is favorite to plasma optical emission. [26]

Bones mainly consist of mineral (60-70 %wt) and organic material (20-30 %wt) parts. Many elements may be present in the mineral phase such as calcium, phosphorus, magnesium, sodium, potassium, chlorine or fluorine. They can be found in the form of carbonate-hydroxyapatite ($Ca_{10}(PO_4)_{6-x}(CO_3)_x(OH)_2$), calcium tribasic phosphate ($Ca_3O_8P_2$), calcium carbonate ($CaCO_3$), calcium fluoride (CaF_2), fluorapatite ($Ca_5(PO_4)_3F$) or magnesium phosphate ($Mg_3(PO_4)_2$). Archaeological bones can also have elements from their surrounding environment such as silicon, iron, aluminum, etc.

In the organic phase (also called ossein), carbon is the key part of carbon dating because it contains the exploitable carbon fraction. Collagen is the main content of organic materials in bones. It is a group of naturally occurring proteins whose molecules are a sequence of amino acids, generally $(Gly\text{-}X\text{-}Y)_n$, or in other words a repeating unit "glycine - amino acid 1 - amino acid 2", while the amino acids X and Y are often proline and hydroxyproline (they represent 15 to 30% of the residues) [27].

Samples Selection and Preparation

According to their conservation statuses, bones undergo different diagenesis mechanisms, which can induce a loss of collagen. The residual collagen content of a bone is thus a good tool for assessing its conservation status. Signals of diatomic molecules as CN or C_2 are often used in organic material analysis using LIBS. Moreover, the spectral lines emission from carbon or nitrogen is also used. In addition, nitrogen in the bones only comes from their organic phase, and almost exclusively from collagen. The nitrogen content of the bones thus indicates the remaining amount of collagen. Bocherens et al. [9] proved that an empirical relationship can reflect the evolution of the carbon and nitrogen contents of a bone that loses its collagen, without the addition of carbon from outside pollution.

$$C\ \%wt = 2.7 \times N\ \%wt + 1.4 \quad (1)$$

By plotting this formula in Figure 1, a relevant calibration curve is obtained and it represents the "status" of the bone in terms of degradation. The nitrogen mass content in the bones varies between 0 and 5%wt. A bone with a content greater than 4%wt is conventionally considered as a "fresh" (Blue zone in Figure 1), a content of less than 1%wt indicates a bone that has undergone significant diagenesis (Yellow zone in Figure 1), and a concentration of less than 0.4%wt shows an absence of collagen (Dark yellow zone in Figure 1). This curve can be also used by entering the nitrogen concentration to evaluate the carbon outside pollution if the carbon concentration is superior to point in the curve.

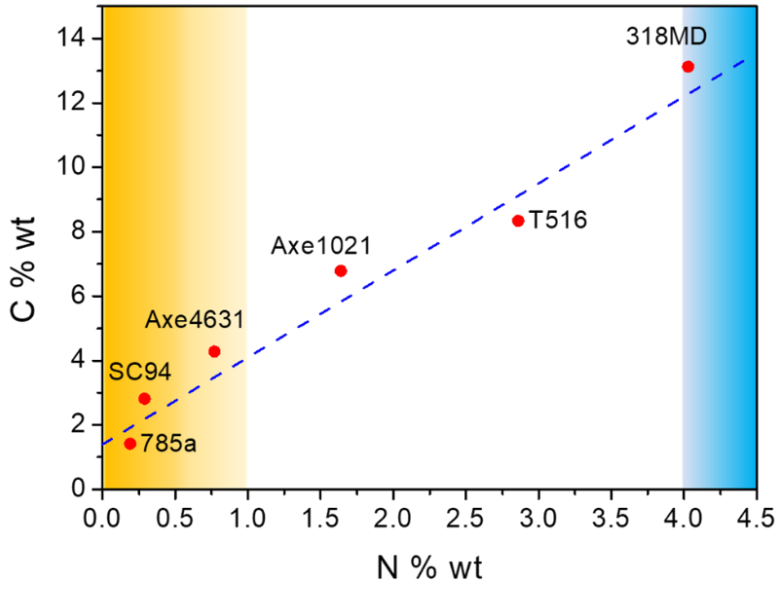

Figure 1. Distribution of bones samples according to their carbon and nitrogen concentration. The dashed line represents the empirical relationship Formula (1).

Six bone samples were selected according to diverse nature, age, and origin in order to analyze representative archaeological bones (Table 1). Their concentration of carbon and nitrogen was measured beforehand with flash combustion coupled with gas chromatography, which was also plotted in Figure 1. The nitrogen and carbon contents of these samples cover the full range of degradation levels [28], and these bones do not feature an obvious outside carbon pollution. Powered bone samples have been obtained by crushing the bones after being cleaned and degreased. The powders were then put into pellets of 6 mm diameter for 2 minutes under a pressure of 1 ton. Except for sample 785a, the raw bones remain available.

Table 1 The information of the examined bones and their nitrogen and carbon concentration of the samples from the flash combustion analysis

Reference	***Type***	***Origin***	***Age ^{14}C (years)***	***C (%wt)***	***N (%wt)***
318MD	Human right hand	Paykend site in Uzbekistan	135±30	13.12	4.03
T516	Human Skeleton	Peyre Clouque site in France	1485±25	8.33	2.86

Axe1021	Camel scapula	Paykend site in Uzbekistan	1100±30	6.78	1.64
Axe4631	Camel scapula	Paykend site in Uzbekistan	940±30	4.28	0.77
SC94	/	Sclayn site in Belgium	/	2.81	0.29
785a*	Human skull	Museum piece	Insufficient collagen	1.41	0.19

(*: no raw bone available, /: unknown)

Experimental Setup and Protocols

A specific experimental setup has been developed to answer this research problem and is presented in Figure 2. A Nd:YAG laser (laser: CFR, Lumibird Quantel, France) provides the fourth harmonic of Nd:YAG laser at 266 nm with a nominal pulse duration of 5.5 ns (FWHM), operated at 20 Hz. The pulse energy was delivered on the sample surface was adjusted and controlled by an attenuator (ATT) and a power meter (not shown in the figure). A mechanical beam shutter controlled the delivery of a single laser pulse per second. The laser beam was focused onto the sample with a lens (L1) of 30 cm focal length (f= 30 cm), inducing a laser-material interaction area of about 120 µm diameter.

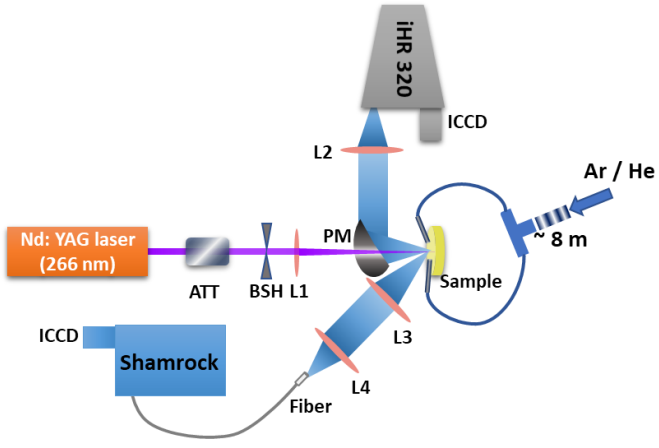

Figure 2 Experimental setup. L1-4: Plano-convex lens, PM: off-axe parabolic mirror, ATT: Attenuator; BSH: mechanical beam shutter.

Two collection paths allowed to collect the plasma emission and to transfer the collected light to two different spectrometers. In the first path, the produced plasma emission was collected by an off-axis parabolic mirror (parallel to focused beam) with a hole to let the laser beam pass through it, and to image the plasma emission with a lens (L2: f=10 cm) at the entrance of a spectrometer. A Czerny-Turner spectrometer (iHR320, HORIBA Scientific, Japan) with three gratings of 300, 1800 and 2400 lines/mm coupled with an ICCD camera (DH340T-18F-E3, Andor Technology, UK). In the second collection path, the emission was collected by a lens (L3: f=15 cm) and transmitted through an optical fiber placed in the image plane of the 4-f imaging system with L3 and L4 (f=10 cm). The fiber was connected to a Czerny-Turner spectrometer (Shamrock 303i, Andor Technology, UK) with three gratings of 600, 1200 and 1800 lines/mm and was coupled to an ICCD camera (DH340T-18F-E3, Andor Technology, UK). Time-resolved detection was performed for spectroscopic measurement by triggering the ICCD camera with the synchronization signal generated by a delay generator. Each spectrum was acquired on a single shot basis and a series of spectra were recorded from the same crater on the sample for one measurement. The selected spectrometer setting corresponding to the observed emission line is shown in Table 2. Due to the large difference in wavelength between carbon atomic emission (C I) at 247.8 nm and nitrogen atomic emission (N I) at approximately 744 nm, it is necessary to use two different spectral zones to have a good resolution.

Table 2 Selected spectral zone for CN violet band ($B^2\Sigma^+ - X^2\Sigma^+$, $\Delta v = 0$), C and N lines emission [29]

	Emission line (nm)	Spectrometer	Spectral zone observation (nm)	Nominal resolution (nm)
CN violet band	388.3, 387.1, 386.2, 385.5, 385.1	Shamrock	382 - 390	0.06
Carbon (C I)	247.8	Shamrock	235 - 262	0.06
Nitrogen (N I)	742.4, 744.2, 746.8	iHR 320	740 - 750	0.06

In order to avoid the influence of nitrogen from ambient air, a flow of gas surrounding the laser impact zone was delivered with a fixed rate of 3 L/min by a pair of tubes (4 mm diameter) installed above the target. Such flow ensured the expansion of the plasma into an environment at atmosphere pressure without the invasion of air. Two types of noble gas were used, Argon and Helium. The gases were mixed into the same tube by a "T-connecter". Either pure or mixture gas propagated in a long tube of a length about 8 m between each bottle and separator into two tubes. This distance allowed the two gases to be mixed homogeneously. The electron density and the temperature of a plasma produced in He environment drop quickly and therefore reduce continuum emission, thus increasing the detection capability of the elemental line in the early life of the plasma. It can also avoid a large broadening caused by dense electron density. Conversely, an Ar environment can raise and maintain a certain plasma's electron density and temperature [30]. Figure 3 shows the effects of ambient gas on plasma emission at the C-N band from the moment when the clear C-N band observed on the sample pellet. The laser fluence was set at 36.3 J/cm^2 and the detection window was kept from 1000 to 3000 ns after the laser pulse arriving at the surface for all C-N band measurement.

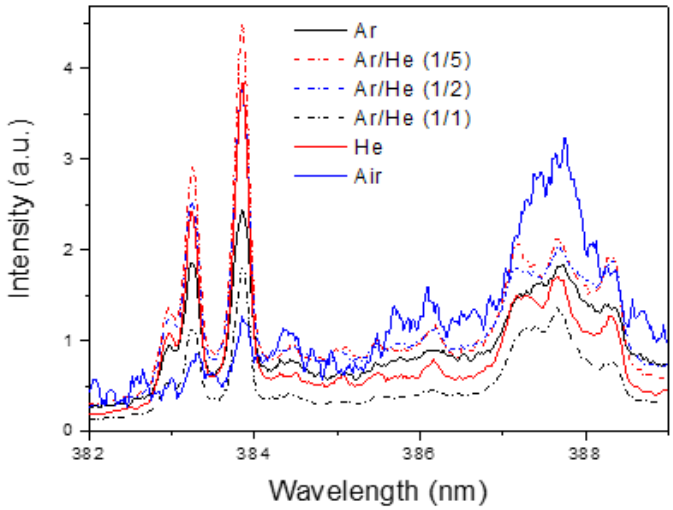

Figure 3 CN band emission from the plasma induced in different ambient gas on T516 pellet. Each spectrum is obtained by averaging 30 spectra acquired at the same crater.

In order to get the best signal to background ratio from the emission, the flux proportion of argon to helium was set to 1:5 of the 3 L/min total flux, which is also proved to favor organic material analysis by LIBS [31]. However, in the spectral zone for N I emission, it is prone to have the emission of Ar I, so for elemental analysis of carbon and nitrogen, the pure He ambient was used. In addition, the laser fluence was raised to 77.8 J/cm^2 to counterbalance the low temperature in the He environment in order to have a strong enough emission for this study. The detection window was changed from 100 to 400 ns after the laser pulse arriving at the surface, which favors elemental emissions.

One typical atomic emission spectrum presenting the lines of carbon and nitrogen from the sample 318MD is shown in Figure 4. In this spectral range, the atomic emission of calcium and phosphorus from the mineral phase of bones can also be collected and measured.

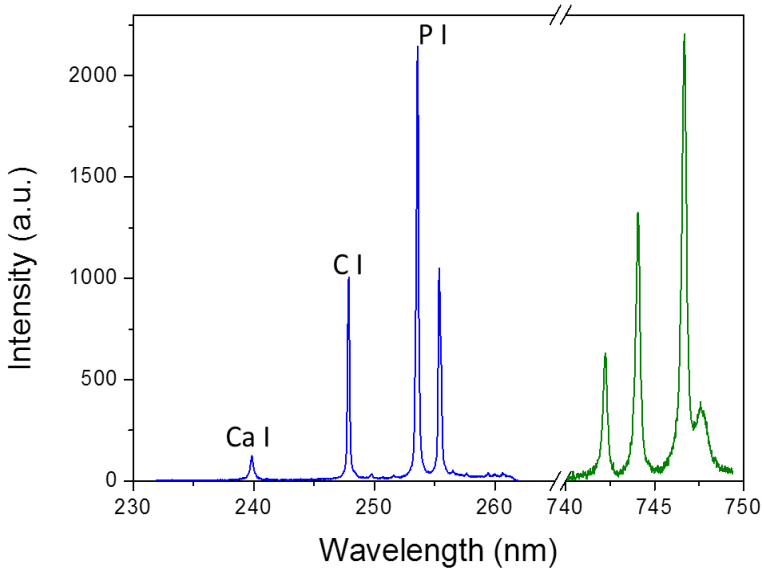

Figure 4 Atomic line emission from the sample 318MD pellet of two spectral ranges: the blue line contains the emission for calcium, carbon and phosphorus, and the green line contains the nitrogen atomic emission.

For pellet sample, 30 spectra were recorded at the same ablation zone. The initial surfaces of raw bone samples often require treatments in order to remove flaws and traces of pollution. The diagenesis process can reduce the hardness of the bone; therefore, we used a pre-cleaned scalpel

remove the first layer of the surface. The advantage of cleaning is not only to remove the pollution but also to provide a relatively flat surface for ablation. In Figure 5, the craters are deeper on the cleaned surface than the raw one after 100 laser shot ablation, which confirms that the cleaned surface is harder because the laser pulse removed more material.

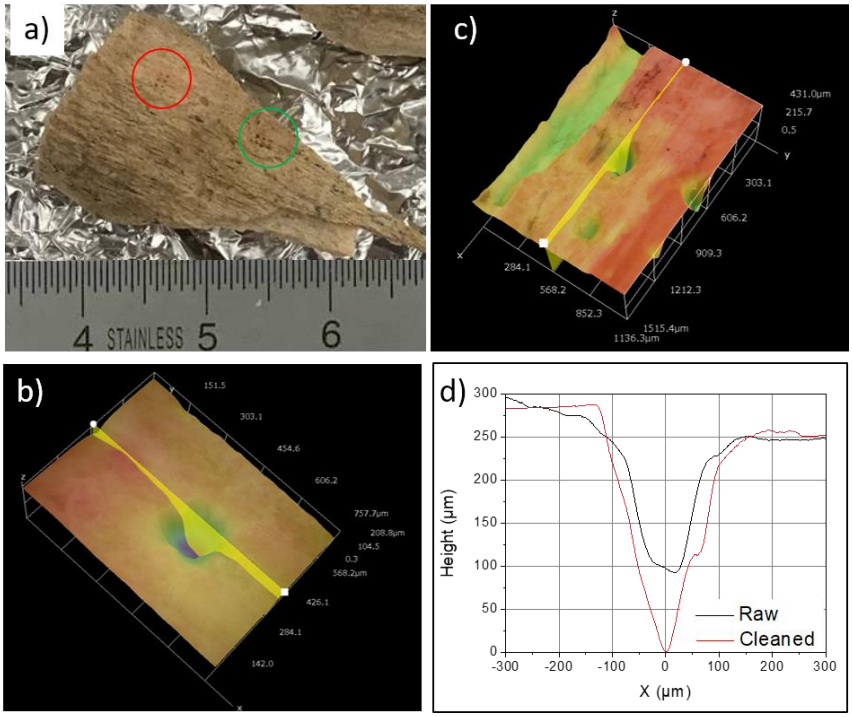

Figure 5 T516 raw bone sample. **a**: raw bone sample, the raw surface (green circle) and the cleaned surface (red circle); Craters ablated at raw surface(**b**) and cleaned surface (**c**) and their profile (**d**).

The 100 spectra obtained from these craters in He environment are arranged as a function of number of laser shot and are shown in Figure 6. The intensity is normalized by its own maximum and represented by false color. In Figure 6 a and b, the first spectra have more emission than the deeper parts. This shows the pollution found at the raw surface. The emission is more stable and shows less interference after cleaning (Figure 6 c-d).

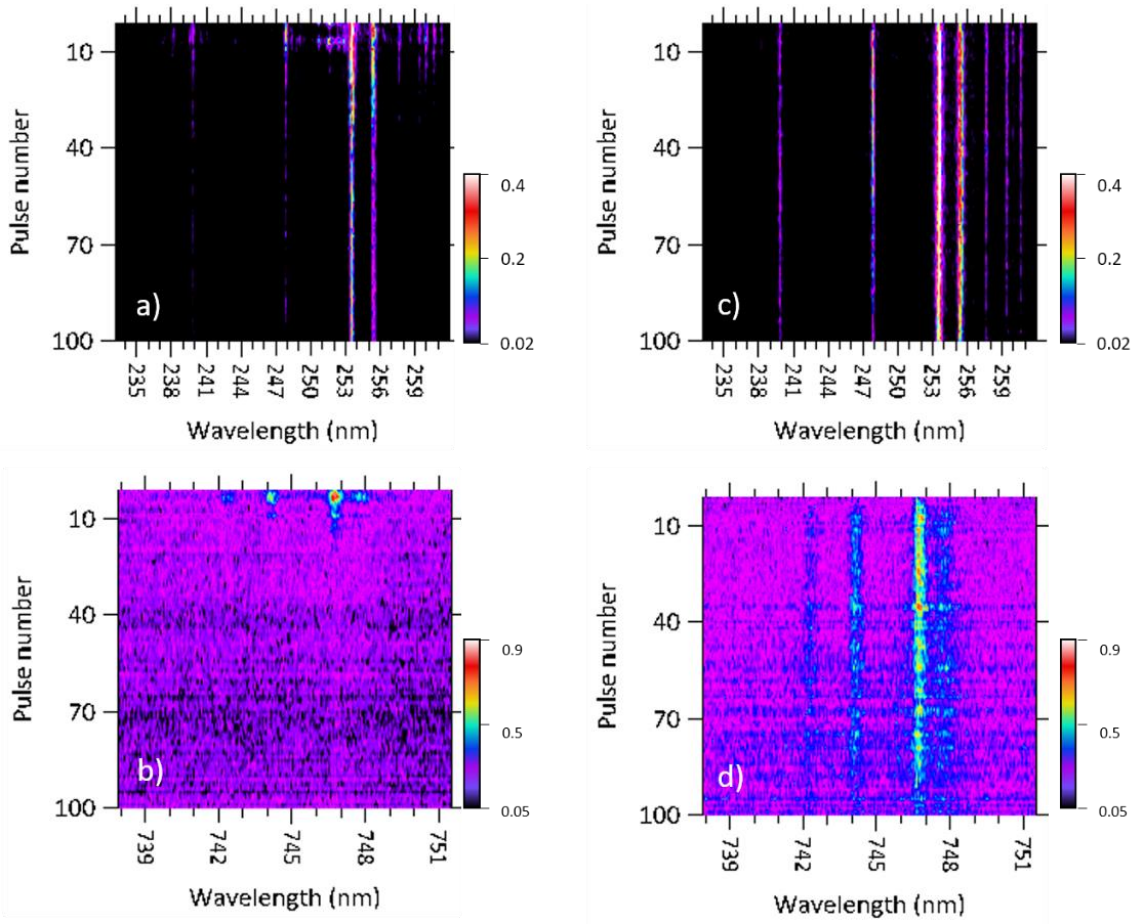

Figure 6 Spectra as a function of number of laser shots from T516 raw bone sample. carbon(**a**) and nitrogen (**b**) spectral zone emission from the raw surface; carbon(**c**) and nitrogen (**d**) spectral zone emission the cleaned surface. In each sub figure, the intensity is normalized by its own maximum.

Figure 7 shows carbon (a-d) and nitrogen (e-h) spectral zone emissions as a function of the number of laser shots on the raw bone samples 318MD, Axe1021, Axe4631, and SC94, respectively. The first 10 spectra were not considered in order to avoid the pollution influence, and the 30 next spectra were selected for analysis.

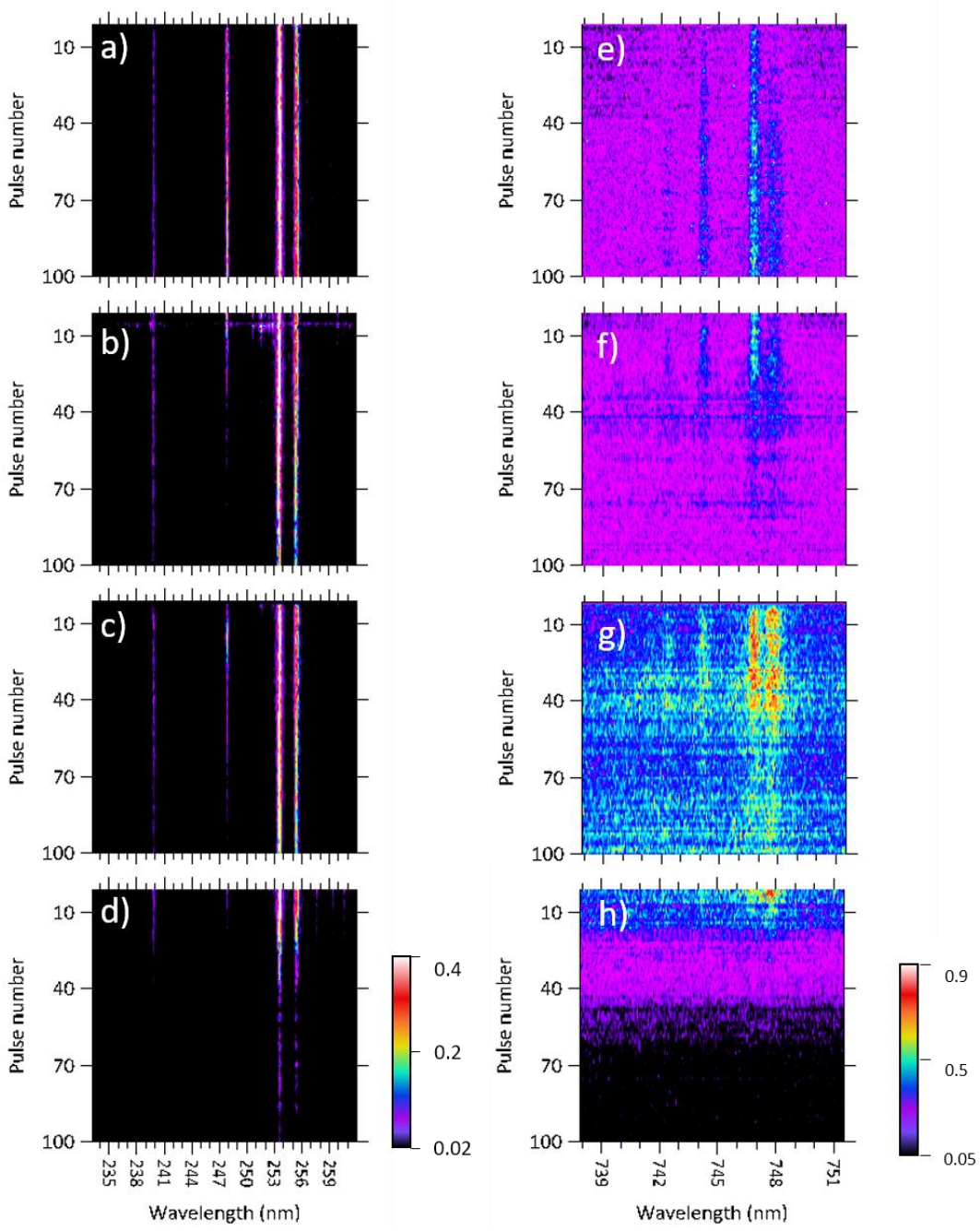

Figure 7 Carbon (**a-d**) and nitrogen (**e-h**) spectral zone emission as a function of the number of laser shot on the raw bone samples, 318MD, Axe1021, Axe4631, and SC94, respectively. The intensity is normalized by its own maximum in each subfigure.

Experimental Results and Discussion

CN band emission from pellet samples in Ar-He mixture environment

In the previously described environment of Ar-He mixture, CN band emissions for the different N concentrations are shown in Figure 8 by arrows indicating the different CN vibrational transition. The emission of 387.1 nm is hidden by the strong Ca emission in this range. The clear CN molecular band emission can be obtained from the sample whose nitrogen concentration is superior to 1%wt. The growing trend of emission intensity follows that of the contained nitrogen. Therefore, the presence of emissions from CN molecules can be the indicator of a sample which did not undergo significant diagenesis.

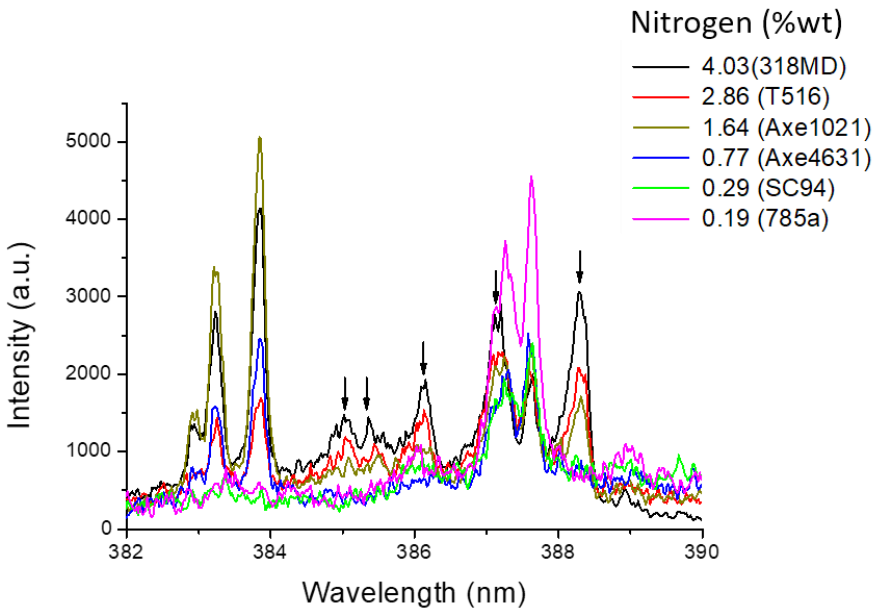

Figure 8 CN band emissions from samples with different N concentrations in a mixture of Ar and He at atmospheric pressure. Each spectrum is obtained by averaging 30 spectra acquired on the same crater.

Helium Gas Experimentation from pellet samples

We recorded the different spectra obtained from the different samples in the spectral range containing N I lines. The Figure 9 presents the superposition of the different spectra and in particular the 744.2 nm line that was used for the calibration. As a result of the ability of Helium

to capture free electrons, the nitrogen lines are well separated without much broadening even at very short delay. We can see that the emission intensity from the N I line of different sample follows the same trend as their nitrogen concentration. The line emission is well detected for the poorest nitrogen concentration, which means that LIBS is a suitable method for this measurement.

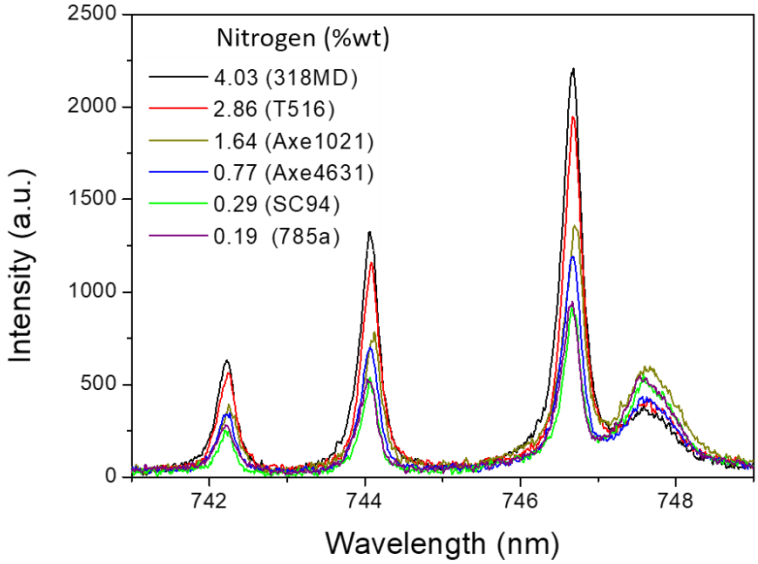

Figure 9 Nitrogen atomic line emissions for bone samples of different N concentration in He environment at atmospheric pressure.

We plotted the emission intensity of N I 744.2 nm as a function of the nitrogen concentration in each sample shown in Figure 10. The fitting curve has a coefficient of determination (R^2) of 0.9684 and its 95% confidence band is shown between two blue dot lines in Figure 10. The N I 744.2 nm line emission intensity of a random bone sample can be plotted in this calibration curve in order to calculate its nitrogen concentration.

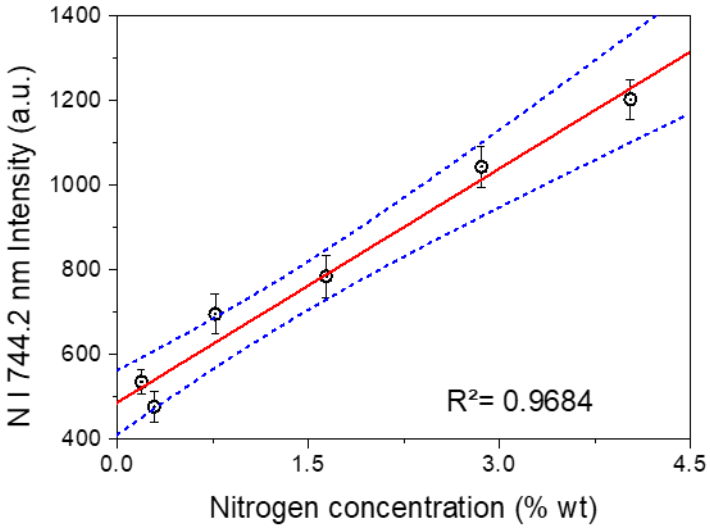

Figure 10 Calibration curve from N I 744.2. The black points show the intensity with 95% confidence interval of the measure statistics (error bar), the red line is the fitting calibrated line and between the blue dot lines shape the 95% confidence bands

The carbon concentration in ancient bones is also an important criterion because it conveys information not only on degradation levels but also on environmental pollution. The C I 247.8 nm line emission intensity is shown in Figure 11a and follows the same tendency as their carbon concentration. The carbon calibration curve (Figure 11b) was obtained following the same procedure as for the nitrogen calibration curve (Figure 10).

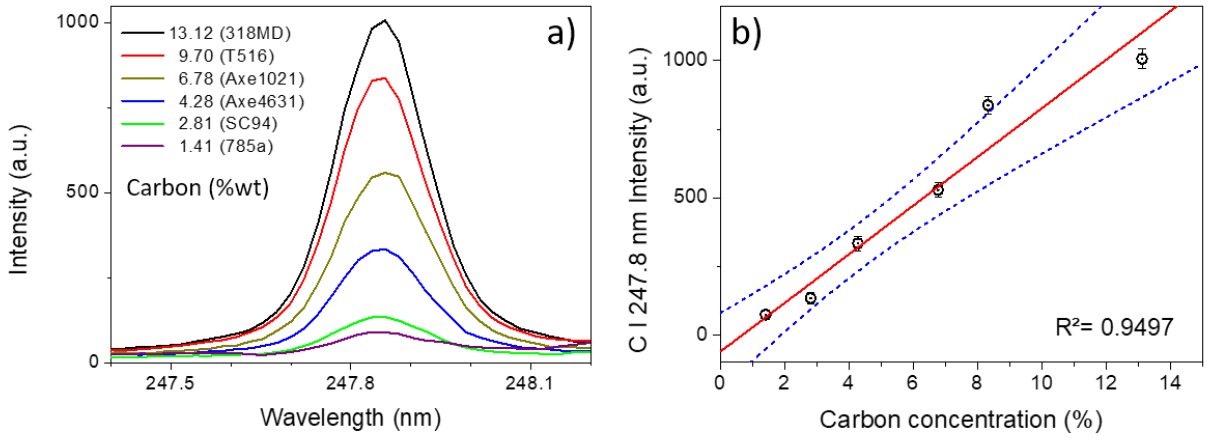

Figure 11 a: Carbon atomic line emission for bone samples of different C concentration in He environment at atmospheric pressure; **b**: Calibration curve from C I 247.9 nm. The black points show the intensity with the error bar, the red line is the fitting calibrated line and between the blue dot lines shape the 95% confidence bands of linear fitting

Knowing that the C concentration has a linear relationship with that of nitrogen, we obtained the linear relation between carbon and nitrogen emission intensities, which is shown in Figure 12 with an R^2=0.9587. Comparing with Figure 1, three areas were separated from each other: the absence of collagen (N% <0.4%wt), the "fresh bones" (N% >4%wt), and the concentration in the middle. The threshold for effective radiocarbon dating (samples that did not undergo significant diagenesis: N% <1 %wt) was well determined by the ability of separating the two samples: Axe4631(N%=0.77%wt) and Axe1021(N%=1.64%wt).

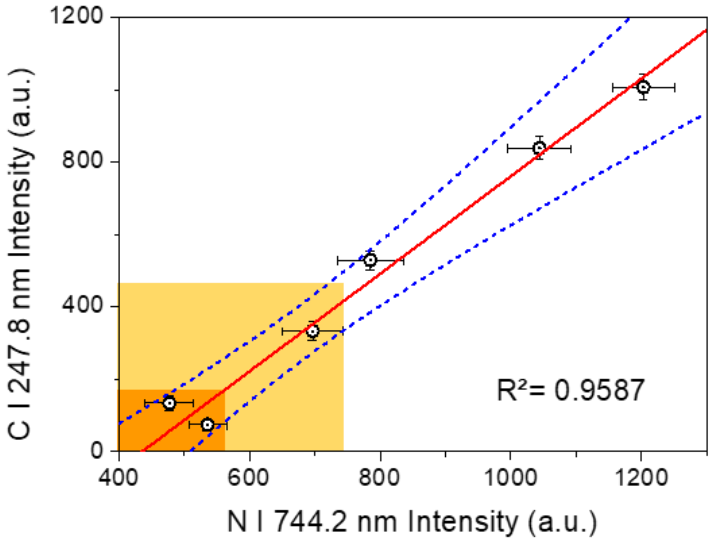

Figure 12 Distribution of C-N intensity. The black points show the intensity with the error bar, the red line is the fitting calibrated line and between the blue dot lines shape the 95% confidence bands of linear fitting

However, in the area of weak intensity, the distribution did not follow the monotone because of the inverse intensity of low nitrogen concentration. In order to remove the disturbance from the laser pulse-to-pulse variation and possible inhomogeneity of the sample, a normalized method (Internal standard method) was used to have a better calibration result [32, 33].

We can deduce the similar intensity of the emission lines of the Ca and P from their same

mineral phase concentration in the bones. In the observed spectral rang, a Ca line at 239.9 nm is present with a transition from upper level (E_k) 5.168 eV to lower level (E_i) 0 eV and 4 phosphorous lines emission. The reference line was determined at P I 255.5 nm (transition from E_k =7.176 eV to E_i =2.324 eV) because it can prevent self-absorption from the fundamental level and a high energy level was recommended for a good correction [34].

The calibration curves of N I 744.2 nm and C I 247.8 nm are shown in Figure 13 a) and b) after normalizing the intensity by P I 255.5 nm. The R^2 was improved to 0.9727, 0.9703 for better calibration fitting results. Moreover, 95% confidence bands were narrower, which provides evidence of a better result of linear fitting. Three areas were separated from each other according to the degree of diagenesis and the low concentration/intensity zone was corrected after normalization. The internal normalization method was therefore chosen for further analyses in order to get better results.

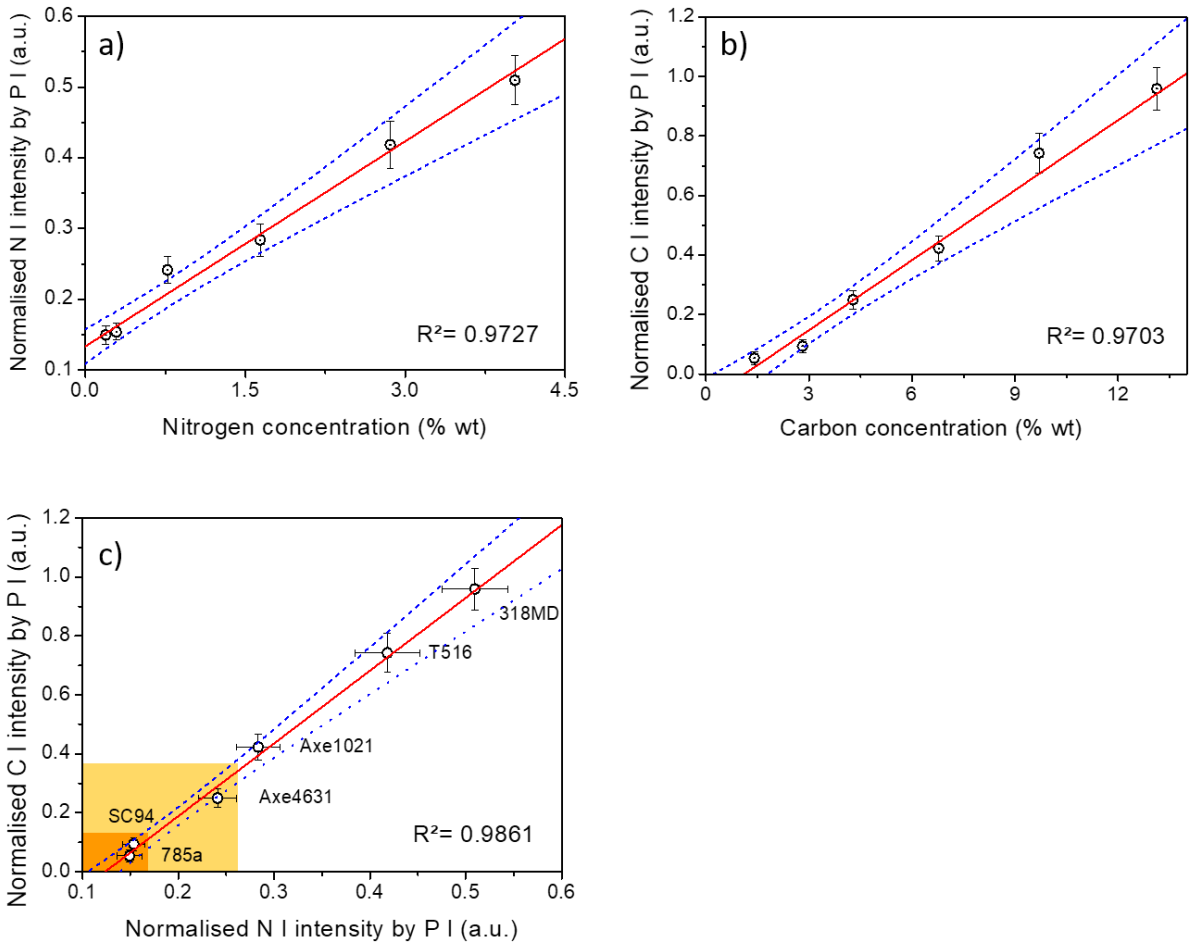

Figure 13 Calibration curves from N I 744.2 nm (**a**) and C I 247.9 nm (**b**) in He after intensity normalization. **c**: Distribution of C-N normalized intensity. The black points show the intensity with the error bar, the red line is the fitting calibrated line and between the blue dot lines shape the 95% confidence bands of linear fitting

Ambient Air Experimentation from pellet samples

It was demonstrated that LIBS enables the prediction of nitrogen and carbon concentrations by plotting a line emission intensity into the calibration curve built under He atmosphere. Despite the fact that nitrogen content from air can contribute to the N I line intensity measured from the plasma emission, working in an air environment still presents practical advantages. This led us to reproduce the experiment under air atmosphere.

If we consider that the N concentration is constant in the air, the contribution of nitrogen from the air in the plasma is also constant. Figure 14a shows a typical spectrum from 318 MD sample in the air in the same detection conditions as in He. The emission line is more broadened in air and the carbon to phosphorous intensity ratio raises. The emission intensity of N I 744.2 nm was plotted as a function of the nitrogen concentration in each sample, as shown in Figure 14b. It should be noted that in Figure 14b, the horizontal coordinate axis should have shifted together with a contribution of nitrogen in the air common to all samples, so the nitrogen concentration from the sample is used to represent the nitrogen concentration value.

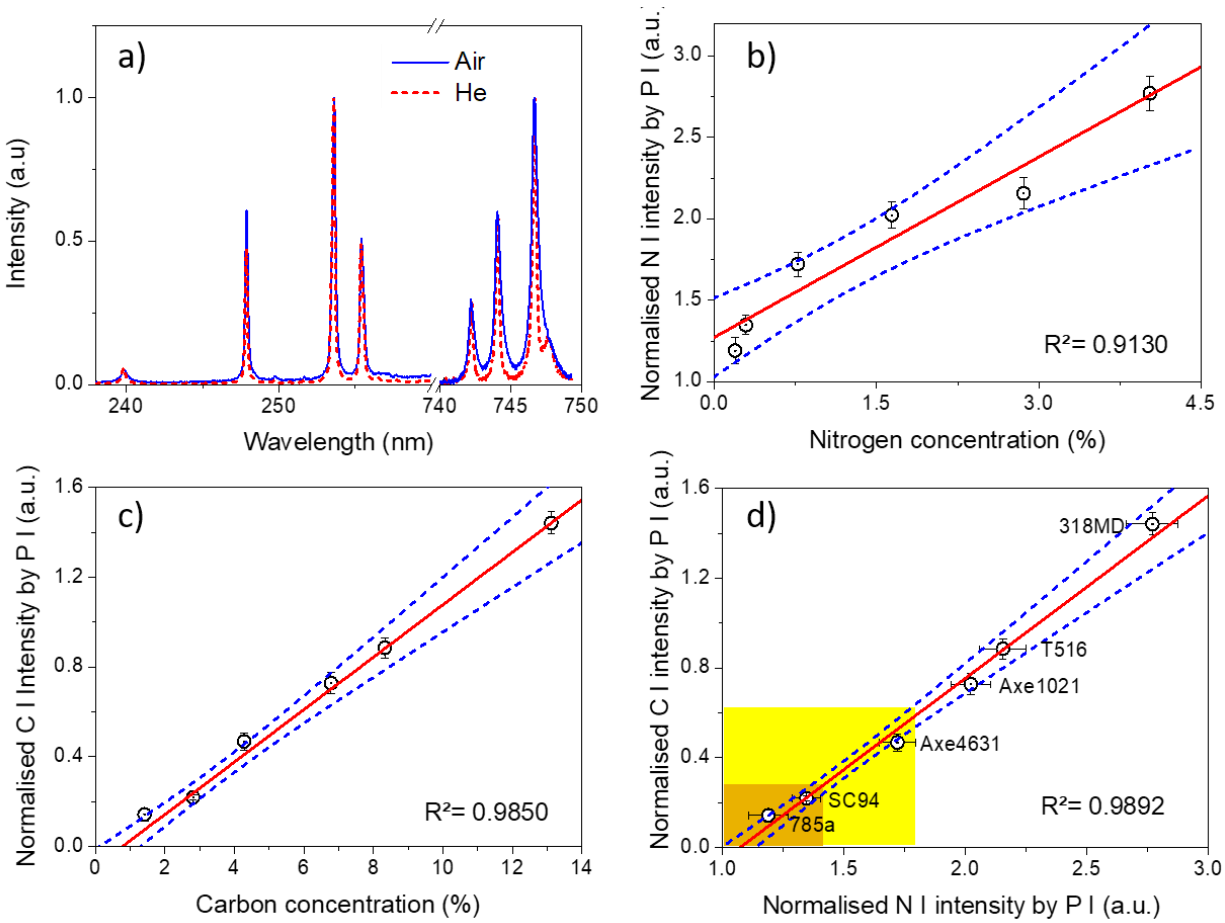

Figure 14 a: Atomic line emission from the sample 318MD in air and He ambient at two spectral ranges: the blue contains the emission for calcium, carbon and phosphorus and the green contains the nitrogen atomic emission; **b**: Calibration curve from N I 744.2 nm

normalized by P I 255.5 nm; **c**: Calibration curve from C I 247.8 nm normalized by P I 255.5 nm. **d**: Distribution of C-N normalized intensity in air. The black points show the intensity with the error bar, the red line is the fitting calibrated line and between the blue dot lines form the 95% confidence bands of linear fitting

A calibration curve was obtained by fitting these emission intensities (red line in Figure 14b). The fitting curve's R^2 is 0.9130 and its 95% confidence bands is shown between two blue dot lines in Figure 14b. This calibration curve showed that although we had a nitrogen contribution from the air in the plasma, the N emission intensity was also following a linear relationship to its concentration in the sample. However, when comparing the 95% confidence bands of linear fitting, the results in air for the low concentration (N% <1%wt) was bigger than that in He.

As a result of N from air, the N I line intensity ratio of the sample with the most nitrogen to the sample with the least was reduced from about 5 to 2. Despite a reduction of the precision due to the air, this calibration curve can also be used to predict N concentration in the future sample

Because all the carbon observable in the plasma originated from the sample, the carbon concentration in the plasma remained the same as in the He environment. The C I line emission intensity is greater in the air than in He, as shown in the Figure 14a. The C I line intensity was also plotted as the function of carbon concentration in the sample in Figure 14c. Its emission intensity is greater in the air with the P I lines. A calibration curve (red line in Figure 14c) was obtained and the R^2 is raised to 0.9850.

We also plotted the C I line intensity as a function of N I line emission intensity (Figure 14d) with a fitting coefficient of determination R^2=0.9892. The comparison between Figure 1 and Figure 14d provides a reliable illustration of the absence of collagen (N% <0.4%wt), of the "fresh bone" (N% >4%wt), and of the threshold for possible radiocarbon dating (N% <1%wt).

The observed results proved the ability of the LIBS technique to perform the evaluation of the remaining collagen concentration in an air environment.

Experimentation from Raw bones

It has been proved in the previous section that LIBS quantitative analysis for the examination of residual amount of collagen is very promising. Transferring this method to the field of archaeology could avoid the sampling work when studying raw bones. Thus, the same examination on raw bones has been carried out. The results from the He environment experimentation are shown in Figure 15.

Because the raw bones are less homogeneous than the pellet sample, the 95% confidence interval of the measure statistics (Error bar) of the intensity is larger in Figure 15 a and b. The calibration curves were nevertheless obtained by fitting N I and C I emission normalized intensities with a fitting coefficient of determination R^2=0.9130 and 0.9501, respectively. This calibration curve showed that although there is an uncertain microscopic structure of bones, the averaged emission intensity was also following a linear relationship with its concentration in the sample.

We also plotted the C I line intensity as a function of N I line emission intensity in Figure 15c with a fitting coefficient of determination R^2=0.9932. The comparison between Figure 1 and Figure 15c provides a reliable illustration of the absence of collagen (N% <0.4%wt), of the "fresh bone" (N% >4%wt), but the threshold for possible radiocarbon dating (N% <1%wt) is uncertain. It may result from of less material being analyzed for each laser pulse, because the mass density is less important than the compressed pellets. The crater volume after 100 laser shot can be estimated by its profile measurement: the diameter is about 200 µm and the depth is about 400 µm from Figure 5c. Therefore, each laser shot ablated about 8 µg with a density of 2 g/cm^3. In contrast with the traditional method of 1-3 g mechanically cleaned bone, LIBS analysis shows the advantage of fewer sample taking.

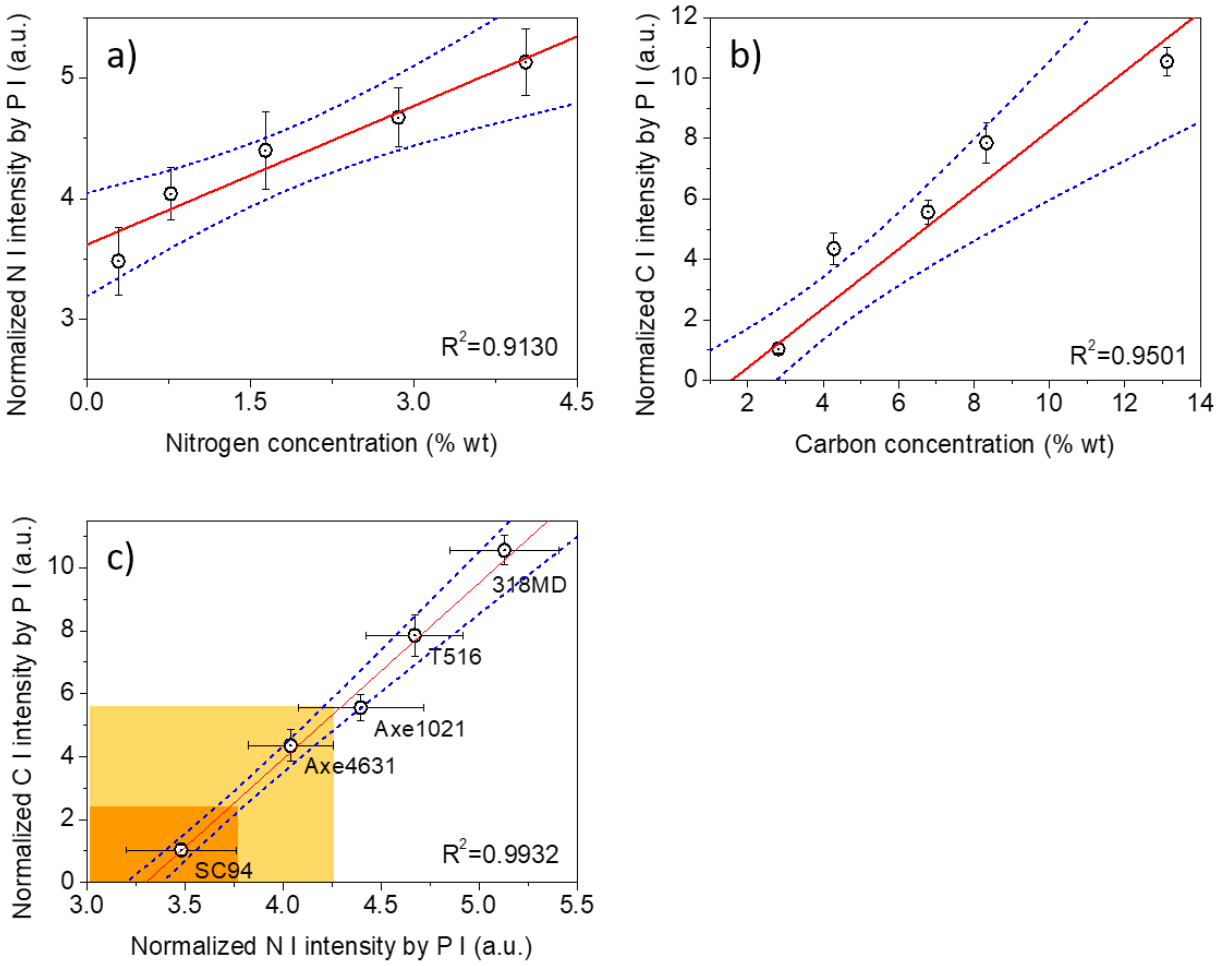

Figure 15 a: Calibration curve from N I 744.2 nm normalized by P I line; Calibration curve from C I 247.8 nm normalized by P I line. **c**: Distribution of C-N normalized intensity, in He for raw bones. The black points show the intensity with the error bar, the red line is the fitting calibrated line and between the blue dot lines is the 95% confidence bands of linear fitting.

The results of raw bones in He environment has proved that LIBS can be applied directly on the raw bones to evaluate the remaining collagen concentration. In order to transfer this measurement to the archeological field, an ideal condition is to carry it out on the raw bones under the ambient air, so the same experiment was also performed in ambient air and the results are shown in Figure 16. As a result of N from air, the N I line emission was stronger than the one in He, and the fluctuation was smaller in this case. Without a He atmosphere catching the free electrons, the plasma is hotter and decays more slowly, which could compensate the

situation of less material emissions. It led to better linear fitting results for both N I and C I calibration. The linear relationship of carbon and nitrogen emission intensity was also found and is shown in Figure 16c.

Unlike the distribution of C-N normalized intensity in He for raw bone, these samples with different remaining collagen content are well separated, which is a reliable illustration of the absence of collagen (N% <0.4%wt), of the "fresh bone" (N% >4%wt), and of the threshold for possible radiocarbon dating (N% <1%wt). The observed results proved the ability of the LIBS technique to perform the evaluation of the remaining collagen concentration from the raw bones in an air environment.

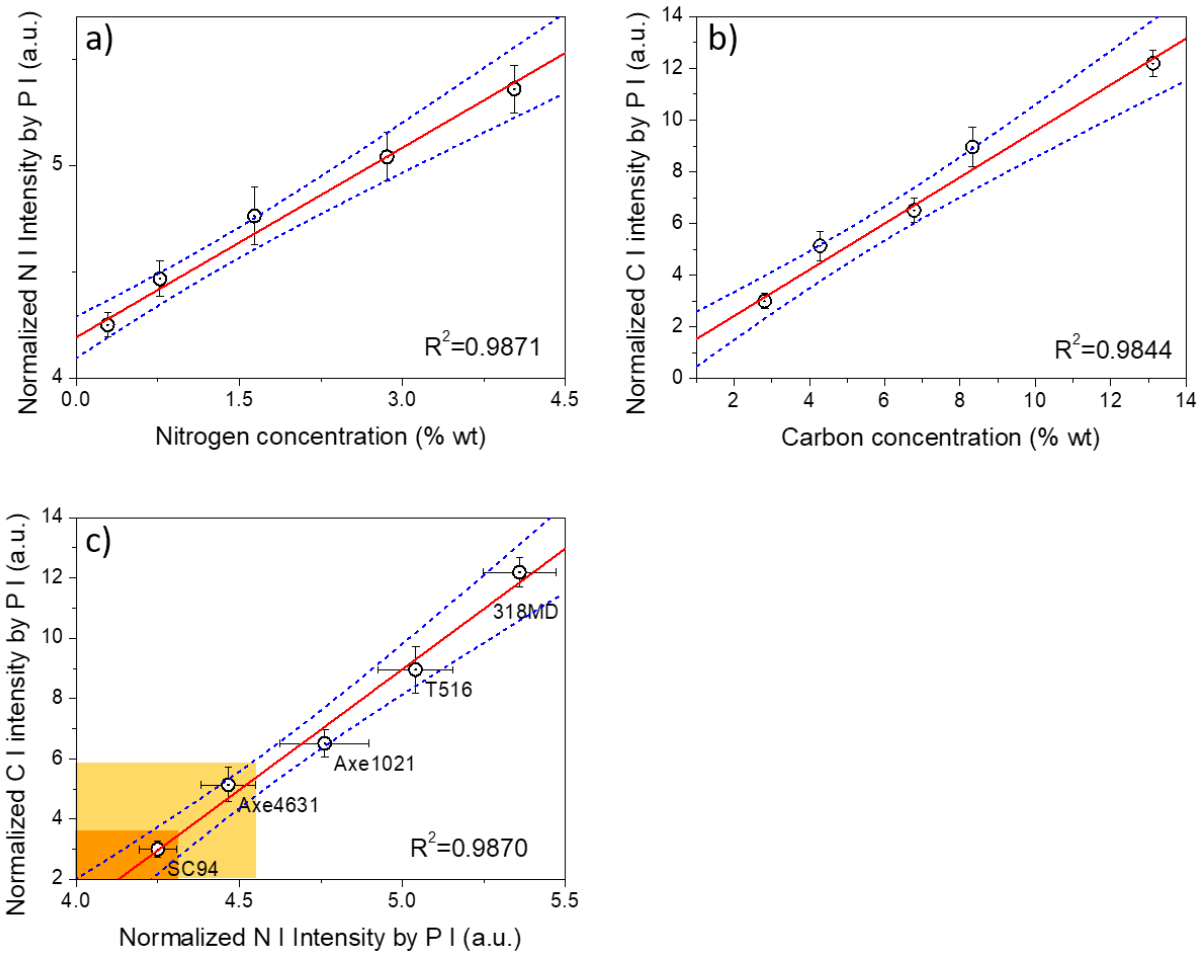

Figure 16 a: Calibration curve from N I 744.2 nm normalized by P I line; **b**: Calibration curve from C I 247.8 nm normalized by P I line. **c**: Distribution of C-N normalized intensity, in air for

raw bones. The black points show the intensity with the error bar, the red line is the fitting calibrated line and between the blue dot lines is the 95% confidence bands of linear fitting.

Conclusion

This work demonstrates the potential of the LIBS technique as an alternative to traditional techniques for the measurement of carbon and nitrogen present in bone collagen, which is a necessary preliminary analysis before performing radiocarbon dating. We first carried out a common method of analyzing the organic material by LIBS by observing C-N band emission in Ar-He mixture environment. The samples that did not undergo significant diagenesis could be well separated for further radiocarbon dating. To achieve a more accurate discrimination, we then studied the relevance of using LIBS to carry out measurements under a Helium atmosphere for isolating the interaction zone in order to exclusively measure the nitrogen from the pellet sample. The calibration curves of carbon and nitrogen were built with a coefficient of determination greater than 0.97, which allowed to perform a quantitative analysis on the tested sample. The linear relationship for the intensity of carbon and nitrogen corresponds to its concentration distribution. The emission intensity can be used to estimate the carbon pollution in the sample. The absence of collagen (N% <0.4 %wt), the "fresh bone" (N% >4 %wt), and the threshold for possible radiocarbon dating (N% <1 %wt) are well determined both in He and air environments. These results are also replicable in an air background, where the carbon calibration curve is well defined. However, it slightly decreases the precision of nitrogen calibration curves. It is therefore recommended to have a controlled environment to carry out this evaluation experiment for a better accuracy of the results, especially for the low collagen content. This method was proven to apply to the field of archaeology in order to avoid the sampling work when studying raw bones. The lost material due to the ablation process is in the magnitude of µg, which proves the micro-destructive nature of the analysis. The performance of this technique can be improved by producing more craters while keeping the total sampling at a

µg level. This study thus establishes why the LIBS quantitative analysis for the examination of residual amount of collagen is very promising, and illustrates that *in situ* rapid LIBS analysis can be a reliable technique for examining if the remaining collagen content is sufficient for radiocarbon dating.

Acknowledgements

This work has been supported by the French Ministry Research Program EquipEx PATRIMEX ANR-11-EQPX-0034 and by the IPERION-CH project funded by the European Commission, H2020- INFRAIA-2014-2015, Grant No. 654028.

Reference

1. J.R. Arnold, W.F. Libby, *Age determinations by radiocarbon content: checks with samples of known age*, ***Science*****, 110** (1949) 678-680.
2. R.E.M. Hedges, I.A. Law, *The radiocarbon dating of bone*, ***Applied Geochemistry***, **4** (1989), 249-253.
3. C Scirè Calabrisotto, M E Fedi, L Caforio, L Bombardieri, P A Mandò, *Collagen quality indicators for radiocarbon dating of bones: New data on bronze age cyprus*, ***Radiocarbon***, **55** (2013) 472-480.
4. R. Longin, *New Method of Collagen Extraction for Radiocarbon Dating*, ***Nature***, **230** (1971) 241-242.
5. N Tisnérat-Laborde, H Valladas, E Kaltnecker, M Arnold, *AMS radiocarbon dating of bones at LSCE****, Radiocarbon,*** **45**(2003) 409-419.
6. R.E.M. HEDGES, *Bone diagenesis: An overview of processes*, ***Archaeometry***, **44** (2002) 319-328.
7. G. J. van Klinken, *Bone Collagen Quality Indicators for Palaeodietary and Radiocarbon Measurements*, ***Journal of Archaeological Science***, **26** (1999) 687-695.
8. R.E.M. Hedges, G. J. Van Klinken, *A review of current approaches in the pretreatment of bone for radiocarbon dating by AMS*, ***Radiocarbon,*** **34**(1992) 279-291
9. H. Bocherens,D. Drucker, D. Billiou, I. Moussa, *Une nouvelle approche pour évaluer l'état de conservation de l'os et du collagène pour les mesures isotopiques (datation au*

radiocarbone, isotopes stables du carbone et de l'azote), ***L'Anthropologie,*** **109**(2005) 557-567.

10. S. H. Ambrose, *Preparation and characterization of bone and tooth collagen for isotopic analysis,* ***Journal of Archaeological Science,*** **17**(1990) 431-451.
11. F. Brock, T. Higham, C. B. Ramsey, *Pre-screening techniques for identification of samples suitable for radiocarbon dating of poorly preserved bones,* ***Journal of Archaeological Science,*** **37**(2010) 855-865.
12. G. Ingram, H. A. C. Montgomery, Joan F. Dymock, G. O. Henneberry, B. E. Baker, J. S. Forbes, D. B. Dalladay and T. W. Bloxam, *The combustion of organic compounds by ignition in oxygen: the determination of carbon and hydrogen,* ***Analyst***, **86**(1961) 411-422.
13. M. Lebon, I. Reiche, X. Gallet, L. Bellot-Gurlet, A. Zazzo, *Rapid quantification of bone collagen content by ATR-FTIR spectroscopy,* ***Radiocarbon,*** **58**(2016) 131-145.
14. Giakoumaki, K. Melessanaki and D. Anglos, *Laser-induced breakdown spectroscopy (LIBS) in archaeological science - applications and prospects,* ***Analytical and Bioanalytical Chemistry,*** **387**(2007) 749-760.
15. V. Spizzichino, R. Fantoni, *Laser Induced Breakdown Spectroscopy in archeometry: A review of its application and future perspectives,* ***Spectrochimica Acta Part B,*** **99** (2014) 201-209.
16. W.Q. Lei, J. El Haddad, V. Motto-Ros, N. Delépine-Gilon, A. Stankova, Q. L. Ma, X. S. Bai, L. J. Zheng, H. P. Zeng , J. Yu, *Comparative measurements of mineral elements in milk powders with laser-induced breakdown spectroscopy and inductively coupled plasma atomic emission spectroscopy,* ***Analytical and Bioanalytical Chemistry,*** **400**(2011) 3303-3313.
17. S. Duchêne, V. Detalle, R. Bruder, and J.B. Sirven, *Chemometrics and laser induced breakdown spectroscopy (libs) analyses for identification of wall paintings pigments,* ***Current Analytical Chemistry,*** **6**(2010) 60-65.
18. R. Bruder, V. Detalle, and C. Coupry, *An example of the complementarity of laser-induced breakdown spectroscopy and raman microscopy for wall painting pigments analysis,* ***Journal of Raman Spectroscopy,*** **38** (2007) 909-915.
19. S. Grégoire, M. Boudinet, F. Pelascini, F. Surma, Y. Holl, V. Motto-Ros, S. Duchêne and V. Detalle, *Laser-induced breakdown spectroscopy (LIBS) for the characterization of organic materials in mural paintings,* ***Lasers in the Conservation of Artworks IX, Archetype Publications Ltd, U.K.*** (2013) 116-124

20. X. Bai, D. Syvilay, N. Wilkie-Chancellier, A. Texier, L.Martinez, S. Serfaty, D. Martos-Levif, V. Detalle, *Influence of ns-laser wavelength in laser-induced breakdown spectroscopy for discrimination of painting techniques*, ***Spectrochimica Acta Part B,* 134** (2017) 81-90
21. S. Grégoire, V. Motto-Ros, Q.L. Ma, W.Q. Lei, X.C. Wang, F. Pelascini, F. Surma, V. Detalle, J. Yu, *Correlation between native bonds in a polymeric material and molecular emissions from the laser-induced plasma observed with space and time resolved imaging*, ***Spectrochimica Acta Part B,* 74-75** (2012)31-37
22. S. Weinerand, H.D. Wagner, *THEMATERIALBONE: Structure-Mechanical Function Relations*, ***Annu.Rev.Mater.Sci*. 28** (1998) 271-298
23. C. Chadefaux, *Etablissement d'une nouvelle stratégie analytique multiéchelle de détermination de l'état de conservation des os et bois de cervidés archéologiques*, **PhD thesis, Université Pierre et Marie Curie**, Paris, 2009
24. J. D. Currey, *The structure and mechanics of bone*, ***Journal of Materials Science,* 47** (2011) 41-54.
25. P. L Blanton and N. L. Biggs. *Density of fresh and embalmed human compact and cancellous bone.* ***American Journal of Physical Anthropology* 29**(2010)39-44.
26. Z A Abdel-Salam, A H Galmed, E Tognoni, et al. *Estimation of calcified tissues hardness via calcium and magnesium ionic to atomic line intensity ratio in laser induced breakdown spectra.* ***Spectrochimica Acta Part B,* 62** (2007)1343-1347.
27. J. A. M. Ramshaw, V. Glattauer, and J. A. Werkmeister, *Collagen,****Encyclopedia of Polymer Science and Technology***, **5**(2003) 603-632.
28. H. Bocherens, D. Drucker, H. Taubald, *Preservation of bone collagen sulphur isotopic compositions in an early Holocene river-bank archaeological site*, ***Palaeogeography, Palaeoclimatology, Palaeoecology*, 310** (2011) 32-38.
29. NIST Atomic Spectra Database: **http://www.nist.gov/pml/data/asd.cfm**
30. J.A. Aguilera, C. Aragon, *A comparison of the temperatures and electron densities of laser-produced plasmas obtained in air, argon, and helium at atmospheric pressure*, ***Applied Physics A*, 69** (1999) S475-S478.
31. R. Bruder, *Etude et développement de la spectroscopie d'émission optique sur plasma induit par laser pour l'analyse de terrain : un exemple d'application aux œuvres d'art*, **PhD thesis ,Université Pierre et Marie Curie**, Paris, 2008
32. S. I. Gornushkin, I. B. Gornushkin, J. M. Anzano, B. W. Smith and J. D. Winefordner, *Effective normalization technique for correction of matrix effects in laser-induced*

breakdown spectroscopy detection of magnesium in powdered samples, ***Applied Spectroscopy,*** **56**(2002) 433-436.

33. Y. Tian, H.C. Cheung, R. Zheng, Q. Ma, Y. Chen, N. Delepine-Gilon, J. Yu, *Elemental analysis of powders with surface-assisted thin film laser-induced breakdown spectroscopy*, ***Spectrochimica Acta Part B,*** **124**(2016) 16-24.
34. N.B. Zorov, A.A. Gorbatenko, T.A. Labutin, A.M. Popov, *A review of normalization techniques in analytical atomic spectrometry with lasers sampling: from single to multivariate correction,* ***Spectrochimica Acta B,*** **65**(2010) 642-657.

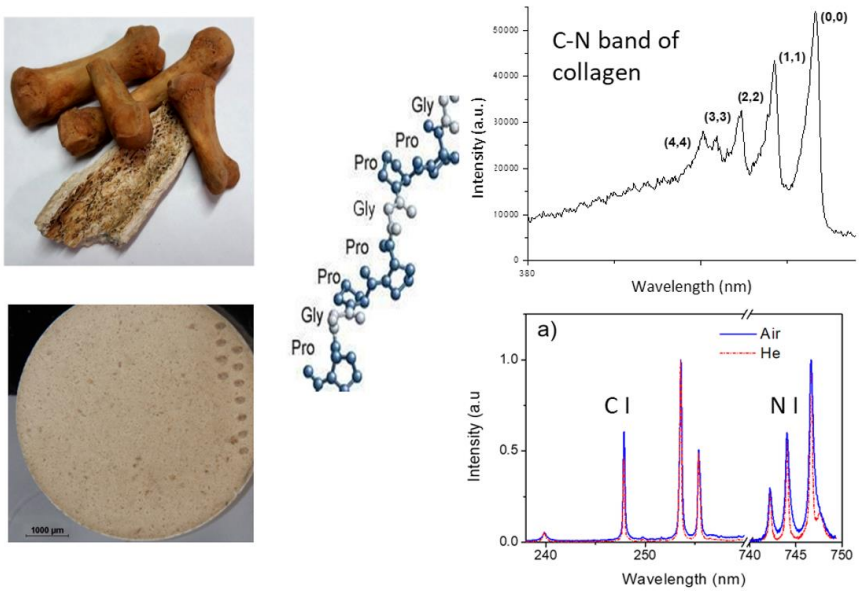

Graphical abstract

Highlights

- First evaluation of the diagenesis rate of ancient bones by LIBS prior to ^{14}C dating
- Quantitative analysis of residual collagen obtained under He environment
- Demonstration of LIBS ability to perform collagen remaining measurement on raw bones
- Determining the residual content of collagen in air for in-field archaeology